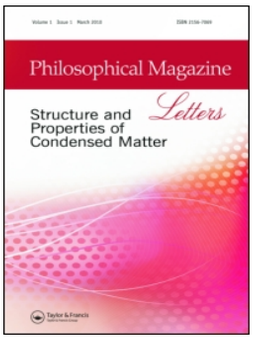

Philosophical Magazine Letters

ISSN: 0950-0839 (Print) 1362-3036 (Online) Journal homepage: https://www.tandfonline.com/loi/tphl20

Affine covariant-contravariant vector forms for the elastic field of parametric dislocations in isotropic crystals

Nasr M. Ghoniem , Jianming Huang & Zhiqiang Wang

To cite this article: Nasr M. Ghoniem , Jianming Huang & Zhiqiang Wang (2002) Affine covariant-contravariant vector forms for the elastic field of parametric dislocations in isotropic crystals, Philosophical Magazine Letters, 82:2, 55-63, DOI: 10.1080/09500830110103216

To link to this article: https://doi.org/10.1080/09500830110103216

Published online: 14 Nov 2010.

Philosophical Magazine Letters, 2002,
Vol. 82, No. 2, 55–63

Taylor & Francis
Taylor & Francis Group

Affine covariant–contravariant vector forms for the elastic field of parametric dislocations in isotropic crystals

Nasr M. Ghoniem†, Jianming Huang and Zhiqiang Wang

Mechanical and Aerospace Engineering Department, University of California
Los Angeles, Los Angeles, California 90095-1597, USA

[*Received 11 June 2001 and accepted 17 September 2001*]

Abstract

The elastic field of closed dislocation loops in isotropic crystals is developed for differential geometric parametric segments in covariant–contravariant vector forms. The displacement vector field, strain and stress tensor fields, as well as the self-energy and mutual interaction energies are all expressed in terms of three covariant basis vectors: the unit tangent **t**, the unit radius **e** and the Burgers vector **b**, and their contravariant reciprocals. Differential affine transformations are shown to map directly the scalar unit interval ($\in [0,1]$) on to vector displacement, and second-rank tensor strain and stress fields of a dislocation segment, described by the parameter ω. The resulting affine differential mappings are independent of coordinate systems and can be readily integrated by analytical or numerical methods to obtain the total field of closed dislocation loops. The method is applied to simplified geometry, where analytical expressions can be obtained and is illustrated in numerical simulations of mesoscopic plastic deformation.

§ 1. Introduction

A relatively recent approach to investigations of mesoscopic plastic deformation is based on direct numerical simulation of the interaction and motion of dislocations. This approach, which is commonly known as dislocation dynamics (DD), was first introduced for two-dimensional (2D) straight, infinitely long dislocation distributions, and then later for a complex three-dimensional (3D) microstructure (for example Kubin and Canara (1992), Hirth *et al.* (1996), Schwarz (1997), and Ghoniem *et al.* (2000)). Since the computational requirements for 3D simulations of plastic deformation are very challenging, it is advantageous to reduce the total number of dislocation segments during such large-scale calculations. However, dislocation configurations at short range can be quite complex because of significant line deformation during short-range interactions (e.g. the formation of junctions and dipoles, annihilation, or interaction with defect clusters). One has therefore two conflicting requirements, where both accuracy and computational speed are determined by the shape of dislocation segments. Recently, we developed and applied a computational method for 3D calculations of mesoscopic plastic deformation (Ghoniem and Sun 1999, Ghoniem *et al.* 2000, 2001), where the elastic field is determined as a fast numerical sum from contributions of curved segments, which are parametrically represented. The field calculations of large dislocation ensembles are used in a

† Email: ghoniem@ucla.edu.

Philosophical Magazine Letters ISSN 0950–0839 print/ISSN 1362–3036 online
http://www.tandf.co.uk/journals
DOI: 10.1080/0950083011010321 6

variational principle to determine the equations of motion of generalized coordinates that are associated with each parametric segment (e.g. the position, tangent and normal vectors at end nodes of each segment). In this letter, we recast the elastic field equations, which we derived earlier (Ghoniem and Sun 1999), in compact and more convenient forms. The current formulation of the elastic field generalizes the idea of parametric dislocations discussed by Sedlaĉek (1997) and Ghoniem *et al.* (2000). Utilization of these forms is demonstrated in two respects. First, a few known cases for the stress field of dislocations of special geometry are analytically derived. Then, we illustrate a numerical application of the method to the computer simulation of mesoscopic plastic deformation of large dislocation ensembles.

§ 2. Formulation

The displacement vector $\mathbf{u}$ and strain $\boldsymbol{\varepsilon}$ and stress $\boldsymbol{\sigma}$ tensor fields of a closed dislocation loop have been given by deWit (1960):

$$u_i = -\frac{b_i}{4\pi}\oint_C A_k \,\mathrm{d}l_k + \frac{1}{8\pi}\oint_C \left(\epsilon_{ikl} b_l R_{,pp} + \frac{1}{1-\nu}\,\epsilon_{kmn} b_n R_{,mi}\right)\mathrm{d}l_k, \tag{1}$$

$$\varepsilon_{ij} = \frac{1}{8\pi}\oint_C \left(-\tfrac{1}{2}\left(\epsilon_{jkl} b_i R_{,l} + \epsilon_{ikl} b_j R_{,l} - \epsilon_{ikl} b_l R_{,j} - \epsilon_{jkl} b_l R_{,i}\right)_{,pp} \frac{\epsilon_{kmn} b_n R_{,mij}}{1-\nu}\right)\mathrm{d}l_k, \tag{2}$$

$$\sigma_{ij} = \frac{\mu}{4\pi}\oint_C \left(\tfrac{1}{2} R_{,mpp}\left(\epsilon_{jmn}\,\mathrm{d}l_i + \epsilon_{imn}\,\mathrm{d}l_j\right) + \frac{1}{1-\nu}\,\epsilon_{kmn}\left(R_{,ijm} - \delta_{ij} R_{,ppm}\right)\mathrm{d}l_k\right) \tag{3}$$

where μ and ν are the shear modulus and Poisson's ratio respectively, $\mathbf{b}$ is the Burgers vector of Cartesian components b_i, and the vector potential $A_k(\mathbf{R}) = \epsilon_{ijk} X_i s_j / [R(R + \mathbf{R}\cdot\mathbf{s})]$ satisfies the differential equation: $\epsilon_{pik} A_{k,p}(\mathbf{R}) = X_i R^{-3}$, where $\mathbf{s}$ is an arbitrary unit vector. The radius vector $\mathbf{R}$ connects a source point on the loop to a field point, as shown in figure 1, with Cartesian components R_i, successive partial derivatives $R_{,ijk\ldots}$ and magnitude R. The line integrals are

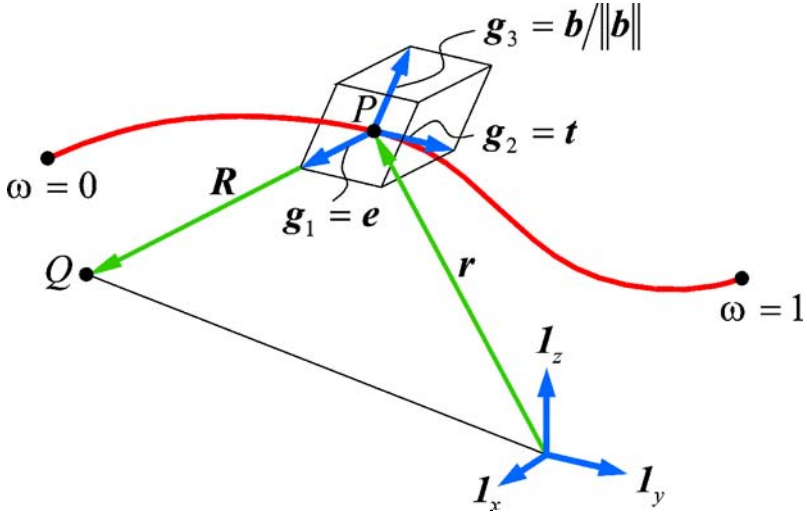

Figure 1. Differential geometry representation of a general parametric curved dislocation segment.

carried along the closed contour C defining the dislocation loop, of differential arc length $\mathrm{d}\mathbf{l}$ of components $\mathrm{d}l_k$. Also, the interaction energy between two closed loops with Burgers vectors $\mathbf{b}_1$ and $\mathbf{b}_2$ respectively can be written as:

$$E_{\mathrm{I}} = -\frac{\mu b_{1i} b_{2j}}{8\pi} \oint_{C^{(1)}} \oint_{C^{(2)}} \left[R_{,kk} \left(\mathrm{d}l_{2j}\, \mathrm{d}l_{1i} + \frac{2\nu}{1-\nu}\, \mathrm{d}l_{2i}\, \mathrm{d}l_{1j} \right) + \frac{2}{1-\nu} \left(R_{,ij} - \delta_{ij} R_{,ll} \right) \mathrm{d}l_{2k}\, \mathrm{d}l_{1k} \right]. \tag{4}$$

The higher-order derivatives $R_{,ij}$ and $R_{,ijk}$ of the radius vector are components of second- and third-order Cartesian tensors respectively, which can be given in the forms

$$\begin{aligned} R_{,ij} &= \left(\delta_{ij} - \frac{X_i}{R} \frac{X_j}{R} \right) \Big/ R, \\ R_{,ijk} &= \left[3\, \frac{X_i}{R} \frac{X_j}{R} \frac{X_k}{R} - \left(\delta_{ij} \frac{X_k}{R} + \delta_{jk} \frac{X_i}{R} + \delta_{ki} \frac{X_j}{R} \right) \right] \Big/ R^2, \end{aligned} \tag{5}$$

where X_i are Cartesian components of $\mathbf{R}$. Substituting $R_{,ij}$ and $R_{,ijk}$ in equations (1)–(4), and considering the contributions only due to a differential vector element $\mathrm{d}\mathbf{l}$, we obtain the differential relationships

$$\mathrm{d}u_i = -\frac{b_i A_k\, \mathrm{d}l_k}{4\pi} + \frac{1}{8\pi R(1-\nu)} \left((1-2\nu) \epsilon_{ikl} b_l\, \mathrm{d}l_k - \frac{1}{R^2}\, \epsilon_{kmn} b_n X_m X_i\, \mathrm{d}l_k \right), \tag{6}$$

$$\begin{aligned} \mathrm{d}\varepsilon_{ij} = \frac{1}{8\pi} \Bigg(& \frac{1}{R^3} \left(\epsilon_{jkl} b_i X_l + \epsilon_{ikl} b_j X_l \right) \mathrm{d}l_k + \frac{3}{R^5(1-\nu)}\, \epsilon_{kmn} b_n X_i X_j X_m\, \mathrm{d}l_k \\ & - \frac{1}{R^3(1-\nu)}\, \epsilon_{kmn} b_n X_m \delta_{ij}\, \mathrm{d}l_k + \frac{\nu}{R^3(1-\nu)}\, \epsilon_{jkl} b_l X_i\, \mathrm{d}l_k + \frac{\nu}{R^3(1-\nu)} \epsilon_{ikn} b_n X_j\, \mathrm{d}l_k \Bigg), \end{aligned} \tag{7}$$

$$\mathrm{d}\sigma_{ij} = \frac{\mu}{4\pi} \frac{1}{R^3} \left[-\epsilon_{jmn} X_m b_n\, \mathrm{d}l_i - \epsilon_{imn} X_m b_n\, \mathrm{d}l_j + \frac{1}{1-\nu} \left(\frac{3}{R^2}\, \epsilon_{kmn} X_m b_n X_i X_j - \epsilon_{kjn} X_i b_n - \epsilon_{kin} X_j b_n + \epsilon_{kmn} X_m b_n \delta_{ij} \right) \mathrm{d}l_k \right]. \tag{8}$$

Figure 1 shows a parametric representation of a general curved dislocation line segment, which can be described by a parameter ω that varies, for example, from 0 to 1 at end nodes of the segment. The segment is fully determined as an affine mapping on the scalar interval $\in [0, 1]$, if we introduce the tangent vector $\mathbf{T}$, the unit tangent vector $\mathbf{t}$, the unit radius vector $\mathbf{e}$ and the vector potential $\mathbf{A}$, as follows:

$$\mathbf{T} = \frac{\mathrm{d}\mathbf{l}}{\mathrm{d}\omega},\ \mathbf{t} = \frac{\mathbf{T}}{|\mathbf{T}|},\ \mathbf{e} = \frac{\mathbf{R}}{R},\ \mathbf{A} = \frac{\mathbf{e} \times \mathbf{s}}{R(1 + \mathbf{e} \cdot \mathbf{s})}$$

The following relations can be readily verified:

$$
\begin{aligned}
A_k\,\mathrm{d}l_k &= \mathbf{A}\cdot\mathbf{T}\,\mathrm{d}\omega \\
&= T\,\mathrm{d}\omega(\mathbf{A}\cdot\mathbf{t}) \\
&= \frac{T\,\mathrm{d}\omega}{R}\,\frac{(\mathbf{e}\times\mathbf{s})\cdot\mathbf{t}}{1+\mathbf{e}\cdot\mathbf{s}}, \\
\epsilon_{ikl}b_l\,\mathrm{d}l_k\mathbf{e}_i &= -\mathbf{b}\times\mathbf{t}, \\
\frac{1}{R^2}\epsilon_{kmn}b_nX_mX_i\,\mathrm{d}l_k\mathbf{e}_i &= -\frac{1}{R^2}\epsilon_{knm}b_nX_mX_i\,\mathrm{d}l_k\mathbf{e}_i \\
&= -\frac{\mathrm{d}\omega}{R^2}[(\mathbf{T}\times\mathbf{b})\cdot\mathbf{R}]\mathbf{R} \\
&= -\mathrm{d}\omega[(\mathbf{T}\times\mathbf{b})\cdot\mathbf{e}]\mathbf{e}, \\
(\epsilon_{jkl}b_iX_l+\epsilon_{ikl}b_jX_l)\,\mathrm{d}l_k\,\mathbf{e}_i\mathbf{e}_j &= \mathbf{b}\otimes(\mathbf{T}\,\mathrm{d}\omega\times\mathbf{R})+(\mathbf{T}\,\mathrm{d}\omega\times\mathbf{R})\otimes\mathbf{b} \\
&= RT\,\mathrm{d}\omega[\mathbf{b}\otimes(\mathbf{t}\times\mathbf{e})+(\mathbf{t}\times\mathbf{e})\otimes\mathbf{b}], \\
\epsilon_{kmn}b_nX_iX_jX_m\,\mathrm{d}l_k\,\mathbf{e}_i\mathbf{e}_j &= [(\mathbf{T}\,\mathrm{d}\omega\times\mathbf{R})\cdot\mathbf{b}]\mathbf{R}\otimes\mathbf{R} \\
&= R^3T\,\mathrm{d}\omega[(\mathbf{t}\times\mathbf{e})\cdot\mathbf{b}]\mathbf{e}\otimes\mathbf{e}, \\
\epsilon_{kmn}b_nX_m\delta_{ij}\,\mathrm{d}l_k\,\mathbf{e}_i\mathbf{e}_j &= [(\mathbf{T}\,\mathrm{d}\omega\times\mathbf{R})\cdot\mathbf{b}]\mathbf{I} \\
&= RT\,\mathrm{d}\omega[(\mathbf{t}\times\mathbf{e})\cdot\mathbf{b}]\mathbf{I}.
\end{aligned}
$$

Let the Cartesian orthonormal basis set be denoted by $\mathbf{1}\equiv\{\mathbf{1}_x,\mathbf{1}_y,\mathbf{1}_z\}$, $\mathbf{I}=\mathbf{1}\otimes\mathbf{1}$ as the second-order unit tensor and $\otimes$ denotes a tensor product. Now define the three vectors ($\mathbf{g}_1=\mathbf{e}$, $\mathbf{g}_2=\mathbf{t}$ and $\mathbf{g}_3=\mathbf{b}/|\mathbf{b}|$) as a covariant basis set for the curvilinear segment, and their contravariant reciprocals as $\mathbf{g}^i\cdot\mathbf{g}_j=\delta^i_j$, where δ^i_j is the mixed Kronecker delta and $V=(\mathbf{g}_1\times\mathbf{g}_2)\cdot\mathbf{g}_3$ is the volume spanned by the vector basis, as shown in figure 1 (Holzapfel 2000). When the previous relationships are substituted back into equations (6)–(8) with $V_1=(\mathbf{s}\times\mathbf{g}_1)\cdot\mathbf{g}_2$, and $\mathbf{s}$ an arbitrary unit vector, we obtain

$$
\begin{aligned}
\frac{\mathrm{d}\mathbf{u}}{\mathrm{d}\omega} &= \frac{|\mathbf{b}||\mathbf{T}|V}{8\pi(1-\nu)R}\left(\frac{(1-\nu)V_1/V}{1+\mathbf{s}\cdot\mathbf{g}_1}\,\mathbf{g}_3+[(1-2\nu)\mathbf{g}^1+\mathbf{g}_1]\right), \\
\frac{\mathrm{d}\boldsymbol{\varepsilon}}{\mathrm{d}\omega} &= -\frac{V|\mathbf{T}|}{8\pi(1-\nu)R^2}[-\nu(\mathbf{g}^1\otimes\mathbf{g}_1+\mathbf{g}_1\otimes\mathbf{g}^1)+(1-\nu)(\mathbf{g}^3\otimes\mathbf{g}_3+\mathbf{g}_3\otimes\mathbf{g}^3) \\
&\quad +(3\mathbf{g}_1\otimes\mathbf{g}_1-\mathbf{I})], \\
\frac{\mathrm{d}\boldsymbol{\sigma}}{\mathrm{d}\omega} &= \frac{\mu V|\mathbf{T}|}{4\pi(1-\nu)R^2}[(\mathbf{g}^1\otimes\mathbf{g}_1+\mathbf{g}_1\otimes\mathbf{g}^1)+(1-\nu)(\mathbf{g}^2\otimes\mathbf{g}_2+\mathbf{g}_2\otimes\mathbf{g}^2) \\
&\quad -(3\mathbf{g}_1\otimes\mathbf{g}_1+\mathbf{I})], \\
\frac{\mathrm{d}^2E_I}{\mathrm{d}\omega_1\,\mathrm{d}\omega_2} &= -\frac{\mu|\mathbf{T}_1||\mathbf{b}_1||\mathbf{T}_2||\mathbf{b}_2|}{4\pi(1-\nu)R}\{(1-\nu)(\mathbf{g}^{\mathrm{I}}_2\cdot\mathbf{g}^{\mathrm{I}}_3)(\mathbf{g}^{\mathrm{II}}_2\cdot\mathbf{g}^{\mathrm{II}}_3)+2\nu(\mathbf{g}^{\mathrm{II}}_2\cdot\mathbf{g}^{I}_3)(\mathbf{g}^{\mathrm{I}}_2\cdot\mathbf{g}^{\mathrm{II}}_3) \\
&\quad -(\mathbf{g}^{\mathrm{I}}_2\cdot\mathbf{g}^{\mathrm{II}}_2)[(\mathbf{g}^{\mathrm{I}}_3\cdot\mathbf{g}^{\mathrm{II}}_3)+(\mathbf{g}^{\mathrm{I}}_3\cdot\mathbf{g}_1)(\mathbf{g}^{\mathrm{II}}_3\cdot\mathbf{g}_1)]\}, \\
\frac{\mathrm{d}^2E_S}{\mathrm{d}\omega_1\,\mathrm{d}\omega_2} &= -\frac{\mu|\mathbf{T}_1||\mathbf{T}_2||\mathbf{b}|^2}{8\pi R(1-\nu)}\{(1+\nu)(\mathbf{g}_3\cdot\mathbf{g}^{\mathrm{I}}_2)(\mathbf{g}_3\cdot\mathbf{g}^{\mathrm{II}}_2)-[1+(\mathbf{g}_3\cdot\mathbf{g}_1)^2](\mathbf{g}^{\mathrm{I}}_2\cdot\mathbf{g}^{\mathrm{II}}_2)\}.
\end{aligned}
\tag{9}
$$

The superscripts I and II in the energy equations are for loops I and II respectively, and $\mathbf{g}_1$ is the unit vector along the line connecting two interacting points on the loops. The self-energy is obtained by taking the limit of half the interaction energy of two identical loops, separated by the core distance. Note that the interaction energy of prismatic loops would be simple, because $\mathbf{g}_3 \cdot \mathbf{g}_2 = 0$. The field equations are affine transformation mappings of the scalar interval neighbourhood $\mathrm{d}\omega$ to the vector $\mathrm{d}\mathbf{u}$ and second-order tensor $\mathrm{d}\boldsymbol{\varepsilon}$ and $\mathrm{d}\boldsymbol{\sigma}$ neighbourhoods respectively, such that $\mathrm{d}\mathbf{u} = \mathbf{U}\,\mathrm{d}\omega$, $\mathrm{d}\boldsymbol{\sigma} = \mathbf{S}\,\mathrm{d}\omega$, $\mathrm{d}\boldsymbol{\varepsilon} = \mathbf{E}\,\mathrm{d}\omega$. The maps are given by the covariant, contravariant and mixed vector and tensor functions

$$\begin{aligned}
\mathbf{U} &= u^i \mathbf{g}_i + u_i \mathbf{g}^i \\
\mathbf{S} &= \text{sym } [\text{Tr } (A^i_{\cdot j}\, \mathbf{g}_i \otimes \mathbf{g}^j)] + A^{11}(3\mathbf{g}_1 \otimes \mathbf{g}_1 - \mathbf{1} \otimes \mathbf{1}), \\
\mathbf{E} &= \text{sym } [\text{Tr } (B^i_{\cdot j} \mathbf{g}_i \otimes \mathbf{g}^j)] + B^{11}(3\mathbf{g}_1 \otimes \mathbf{g}_1 + \mathbf{1} \otimes \mathbf{1}).
\end{aligned} \tag{10}$$

The scalar metric coefficients $u_i, u^i, A^i_{\cdot j}, B^i_{\cdot j}, A^{11}$ and B^{11} are obtained by direct reduction of equation (9) into equation (10).

§ 3. Applications

3.1. *Analytical*

In some simple geometry of Volterra-type dislocations, special relations between $\mathbf{b}, \mathbf{e}$ and $\mathbf{t}$ can be obtained, and the entire dislocation line can also be described by one single parameter. In such cases, one can obtain the elastic field by proper choice of the coordinate system, followed by straightforward integration. Solution variables for the stress fields of infinitely long pure and edge dislocations are given in table 1, while those for the stress field along the $\mathbf{1}_z$ direction for circular prismatic and shear loops are shown in table 2. The corresponding variables are defined in figure 2 for infinitely straight dislocations, and figure 3 for circular dislocation loops. Note that, for the case of a pure screw dislocation, one has to consider the product of V and the contravariant vectors together, since $V = 0$. When the parametric equations are integrated over z from $-\infty$ to $+\infty$ for the straight dislocations, and over θ from 0 to 2π for circular dislocations, one obtains the entire stress field in dyadic notation as follows.

For an infinitely long screw dislocation,

$$\boldsymbol{\sigma} = \frac{\mu b}{2\pi r}\left(-\sin\theta\, \mathbf{1}_x \otimes \mathbf{1}_z + \cos\theta\, \mathbf{1}_y \otimes \mathbf{1}_z + \cos\theta\, \mathbf{1}_z \otimes \mathbf{1}_y - \sin\theta\, \mathbf{1}_z \otimes \mathbf{1}_x\right). \tag{11}$$

For an infinitely long edge dislocation,

$$\begin{aligned}
\boldsymbol{\sigma} = -\frac{\mu b}{2\pi(1-\nu)r}\big\{&\sin\theta\,[2 + \cos(2\theta)]\mathbf{1}_x \otimes \mathbf{1}_x - [\sin\theta\cos(2\theta)]\mathbf{1}_y \otimes \mathbf{1}_y \\
&+ (2\nu\sin\theta)\mathbf{1}_z \otimes \mathbf{1}_z - [\cos\theta\cos(2\theta)](\mathbf{1}_x \otimes \mathbf{1}_y + \mathbf{1}_y \otimes \mathbf{1}_x)\big\}.
\end{aligned} \tag{12}$$

For a circular shear loop (evaluated on the $\mathbf{1}_z$ axis),

$$\boldsymbol{\sigma} = \frac{\mu b r^2}{4(1-\nu)(r^2+z^2)^{5/2}}\left[(\nu-2)(r^2+z^2) + 3z^2\right](\mathbf{1}_x \otimes \mathbf{1}_z + \mathbf{1}_z \otimes \mathbf{1}_x). \tag{13}$$

Table 1. Variables for screw and edge dislocations.

	Screw dislocation	Edge dislocation
$\mathbf{g}_1(\mathbf{e})$	$\frac{1}{R}(r\cos\theta\,\mathbf{1}_x + r\sin\theta\,\mathbf{1}_y + z\,\mathbf{1}_z)$	$\frac{1}{R}(r\cos\theta\,\mathbf{1}_x + r\sin\theta\,\mathbf{1}_y + z\,\mathbf{1}_z)$
$\mathbf{g}_2(\mathbf{t})$	$\mathbf{1}_z$	$\mathbf{1}_z$
$\mathbf{g}_3(\mathbf{b})$	$b\mathbf{1}_z$	$b\mathbf{1}_x$
$\mathbf{g}^1$	0	$\frac{1}{V}\mathbf{1}_y$
$\mathbf{g}^2$	$\frac{br}{V(r^2+z^2)^{1/2}}(-\sin\theta\,\mathbf{1}_x + \cos\theta\,\mathbf{1}_y)$	$\frac{1}{V(r^2+z^2)^{1/2}(-z\mathbf{1}_y + r\sin\theta\,\mathbf{1}_z)}$
$\mathbf{g}^3$	$\frac{r}{V(r^2+z^2}{}^{1/2}(\sin\theta\,\mathbf{1}_x - \cos\theta\,\mathbf{1}_y)$	$\frac{r}{V(r^2+z^2)^{1/2}}(\sin\theta\,\mathbf{1}_x - \cos\theta\,\mathbf{1}_y)$
$\mathbf{T}$	$\frac{\mathrm{d}z}{\mathrm{d}\omega}\mathbf{1}_z$	$\frac{\mathrm{d}z}{\mathrm{d}\omega}\mathbf{1}_z$
R	$(r^2+z^2)^{1/2}$	$(r^2+z^2)^{1/2}$
V	0	$\frac{br\sin\theta}{(r^2+z^2)^{1/2}}$

Table 2. Variables for circular shear and prismatic loops.

	Shear loop	Prismatic loop
$\mathbf{g}_1(\mathbf{e})$	$\frac{1}{(r^2+z^2)^{1/2}}(r\cos\theta\,\mathbf{1}_x + r\sin\theta\,\mathbf{1}_y + z\,\mathbf{1}_z)$	$\frac{1}{(r^2+z^2)^{1/2}}(r\cos\theta\,\mathbf{1}_x + r\sin\theta\,\mathbf{1}_y + z\,\mathbf{1}_z)$
$\mathbf{g}_2(\mathbf{t})$	$-\sin\theta\,\mathbf{1}_x + \cos\theta\,\mathbf{1}_y$	$-\sin\theta\,\mathbf{1}_x + \cos\theta\,\mathbf{1}_y$
$\mathbf{g}_3(\mathbf{b})$	$b\mathbf{1}_x$	$b\mathbf{1}_z$
$\mathbf{g}^1$	$-\frac{b\cos\theta}{V}\mathbf{1}_y$	$\frac{1}{V}(\cos\theta\,\mathbf{1}_x + \sin\theta\,\mathbf{1}_y)$
$\mathbf{g}^2$	$\frac{1}{V(r^2+z^2)^{1/2}}(-z\,\mathbf{1}_y + r\sin\theta\,\mathbf{1}_z)$	$\frac{br}{V(r^2+z^2)^{1/2}}(-\sin\theta\,\mathbf{1}_x + \cos\theta\,\mathbf{1}_y)$
$\mathbf{g}^3$	$\frac{1}{V(r^2+z^2)^{1/2}}(-z\cos\theta\,\mathbf{1}_x - z\sin\theta\,\mathbf{1}_y + r\,\mathbf{1}_z)$	$\frac{1}{V(r^2+z^2)^{1/2}}(-z\cos\theta\,\mathbf{1}_x - z\sin\theta\,\mathbf{1}_y + r\,\mathbf{1}_z)$
$\mathbf{T}$	$-r\sin\theta\frac{\mathrm{d}\theta}{\mathrm{d}\omega}\mathbf{1}_x + r\cos\theta\frac{\mathrm{d}\theta}{\mathrm{d}\omega}\mathbf{1}_y$	$-r\sin\theta\frac{\mathrm{d}\theta}{\mathrm{d}\omega}\mathbf{1}_x + r\cos\theta\frac{\mathrm{d}\theta}{\mathrm{d}\omega}\mathbf{1}_y$
R	$(r^2+z^2)^{1/2}$	$(r^2+z^2)^{1/2}$
V	$-\frac{bz\cos\theta}{(r^2+z^2)^{1/2}}$	$\frac{br}{(r^2+z^2)^{1/2}}$

For a circular prismatic loop (evaluated on the $\mathbf{1}_z$ axis),

$$\sigma = \frac{\mu b r^2}{4(1-\nu)(r^2+z^2)^{5/2}}\{[2(1-\nu)(r^2+z^2) - 3r^2][\mathbf{1}_x \otimes \mathbf{1}_x + \mathbf{1}_y \otimes \mathbf{1}_y] - 2(4z^2+r^2)[\mathbf{1}_z \otimes \mathbf{1}_z]\}. \tag{14}$$

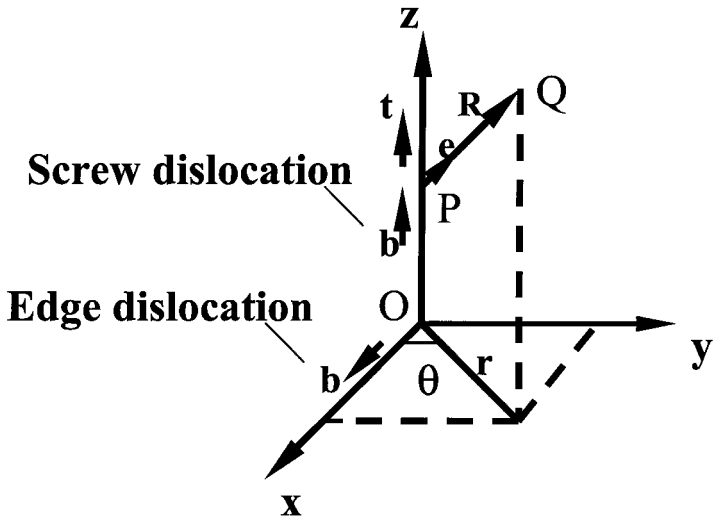

Figure 2. Geometry and variables for infinitely long screw and edge dislocations.

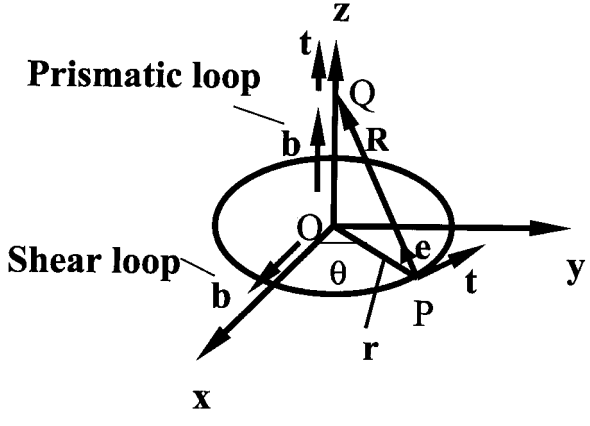

Figure 3. Geometry and variables for circular shear and prismatic loops.

As an application of the method in calculations of self-energy and interaction energy between dislocations, we consider here two simple cases. Firstly, the interaction energy between two parallel screw dislocations of length L and with a minimum distance ρ between them is obtained by making the following substitutions in equation (9):

$$\mathbf{g}_2^{\mathrm{I}} = \mathbf{g}_2^{\mathrm{II}} = \mathbf{g}_3^{\mathrm{I}} = \mathbf{g}_3^{\mathrm{II}} = \mathbf{1}_z, \quad |\mathbf{T}| = \frac{\mathrm{d}l}{\mathrm{d}z} = 1, \quad \mathbf{1}_z \cdot \mathbf{g}_1 = \frac{z_2 - z_1}{[\rho^2 + (z_2 - z_1)^2]^{1/2}},$$

where z_1 and z_2 are distances along $\mathbf{1}_z$ on dislocations 1 and 2 respectively, connected along the unit vector $\mathbf{g}_1$. The resulting scalar differential equation for the interaction energy is

$$\frac{\mathrm{d}^2 E_{\mathrm{I}}}{\mathrm{d}z_1\,\mathrm{d}z_2} = -\frac{\mu b^2}{4\pi(1-\nu)}\left(\frac{\nu}{[\rho^2+(z_2-z_1)^2]^{1/2}} - \frac{(z_2-z_1)^2}{[\rho^2+(z_2-z_1)^2]^{3/2}}\right). \tag{15}$$

Integration of equation (15) over a finite length L yields identical results with those obtained by deWit (1960), and by application of the more standard Blin formula (Hirth and Lothe 1982). Secondly, the interaction energy between two coaxial prismatic circular dislocations with equal radius can be easily obtained by the following substitutions:

$$\mathbf{g}_3^{\mathrm{I}} = \mathbf{g}_3^{\mathrm{II}} = \mathbf{1}_z, \quad \mathbf{g}_2^{\mathrm{I}} = -\sin\varphi_1\,\mathbf{1}_x + \cos\varphi_1\,\mathbf{1}_y, \quad \mathbf{g}_2^{\mathrm{II}} = -\sin\varphi_2\,\mathbf{1}_x + \cos\varphi_2\,\mathbf{1}_y,$$

$$\mathbf{1}_z\cdot\mathbf{g}_2^{\mathrm{I}} = 0, \quad R^2 = z^2 + \left[2\rho\,\sin\left(\frac{\varphi_1-\varphi_2}{2}\right)\right]^2, \quad \mathbf{1}_z\cdot\mathbf{g}_1 = \frac{z}{R}.$$

Integration over the variables φ_1 and φ_2 from 0 to 2π yields the interaction energy, which can be verified to be identical with the form obtained by deWit (1960), and by application of Blin's formula (Hirth and Lothe 1982). Details of all integrations in this letter can be readily verified or checked in the textbook by Walgraef and Ghoniem (2002).

3.2. *Numerical problems*

The vector forms in equation (9) can be integrated for complex-shape loop ensembles, by application of the fast sum method (Ghoniem and Sun 1999). In typical DD computer simulations, the shape of loop ensembles is evolved using equations of motion for generalized coordinates representing the position, tangent and normal vectors of nodes on each loop (Ghoniem *et al.* 2000, 2001). Figure 4 shows the results of such computations for simulation of plastic deformation in single-crystal copper under the action of a slow stress ramp. The initial dislocation density $\rho = 2\times10^{13}$ m^{-2} has been divided into 68 complete loops, of average side length $l_{\mathrm{a}} = 1/\rho^{1/2}$. Each loop contains a random number of straight glide and super-

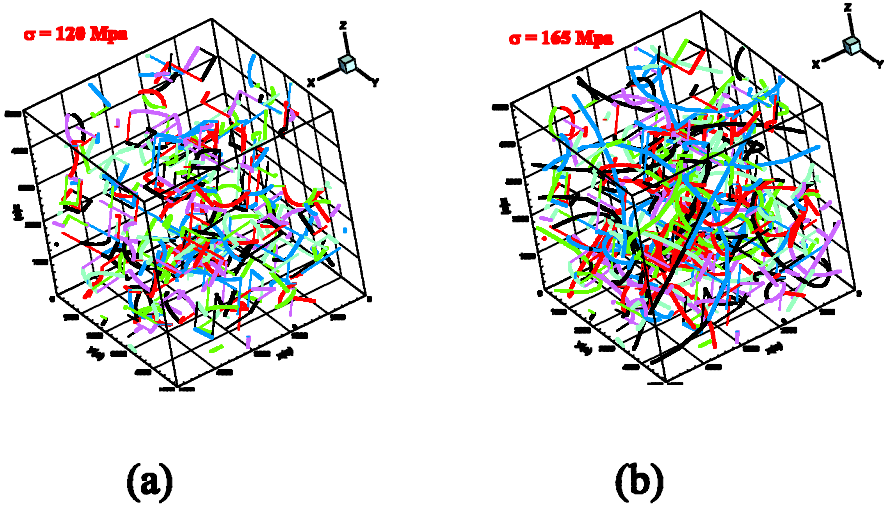

Figure 4. Dislocation loop microstructure for an initial density of 10^{13} m^{-2}, and corresponding to applied stresses σ_{11} of (*a*) 120 MPa, and (*b*) 165 MPa.

jog segments. When a generated or expanding loop intersects the simulation volume of 3 μm side length, the segments that lie outside the simulation boundary are periodically mapped inside the simulation volume to preserve translational strain invariance, without loss of dislocation lines. The initially straight segmented dislocation microstructure evolves under an applied stress $\sigma_{11} = 120$ MPa in figure 4 (*a*) and 165 MPa in figure 4 (*b*). Superjogs (shown as thin lines) are sessile, while glide segments expand considerably under the action of applied stress.

§ 4. Conclusions

The elastic field of arbitrary shape parametric dislocation loops and loop ensembles is determined on the basis of differential geometry representation of covariant–contravariant vector bases that are linked to the parametric shape of piecewise segmented loops. Determination of the vector displacement and stress and strain tensor fields is independent of the coordinate system. These forms can be utilized in analytical verifications by judicious choice of the coordinate system and are also advantageous for large-scale computer simulations of mesoscopic plastic deformation because of their simple and vectorial form. Instead of third-rank tensor components in the stress and strain fields (for example Ghoniem and Sun (1999)) and second-rank tensor components in the interaction energy fields (for example Ghoniem and Sun (1999)) and second-rank tensor components in the interaction energy (for example Hirth and Lothe (1982) and Kubin and Kratochvil (2000)), one uses tensor and dot products respectively of these vectors.

Acknowledgements

This research is supported by the US Department of Energy, Office of Fusion Energy Sciences, through grant DE-FG03-00ER54594, and the US National Science Foundation through grant DMR-0113555 with University of California, Los Angeles.

References

deWit, R., 1960, *Solid St. Phys.*, **10**, 269.
Ghoniem, N. M., and Sun, L. Z., 1999, *Phys. Rev.* B, **60**, 128.
Ghoniem, N. M., Tong, S-.S., and Sun, L. Z., 2000, *Phys. Rev.* B, **139**, 913.
Ghoniem, N. M., Tong, S-.S., Singh, B. N., and Sun, L. Z., 2001, *Phil. Mag.* A, **81**, 2743.
Hirth, J. P., and Lothe, J., 1982, *Theory of Dislocations*, second editions (New York: McGraw-Hill).
Hirth, J. P., Rhee, M., and Zbib, H. M., 1996, *J. Comput.-Aided Mater. Des.*, **3**, 164.
Holzapfel, G., 2000, *Nonlinear Solid Mechanics* (Chichester, West Sussex: Wiley), p. 36.
Kubin, L. P., and Canova, G., 1992, *Scripta metall.*, **27**, 957.
Kubin, L. P., and Kratochvil, J., 2000, *Phil. Mag.* A, **80**, 201.
Schwarz, K. W., 1997, *Phys. Rev. Lett.*, **78**, 4785.
Sedlaček, R., 1997, *Phil. Mag. Lett.*, **76**, 275.
Walgraef, D., and Ghoniem, N., 2002, *Instabilities in Non-equilibrium Materials* (Delft, Kluwer) (to be published).